Hindawi
Advances in Civil Engineering
Volume 2018, Article ID 9286758, 8 pages
https://doi.org/10.1155/2018/9286758

Research Article

Research on the Law of Large-Scale Deformation and Failure of Soft Rock Based on Microseismic Monitoring

Feng Chen,[1] Tianhui Ma,[1] Chun'an Tang,[1,2] Yanhong Du,[3] Zhichao Li,[1] and Fei Liu[1]

[1]*School of Civil Engineering, Dalian University of Technology, Dalian 116024, China*
[2]*State Key Laboratory of Coastal and Offshore Engineering, Dalian University of Technology, Dalian 116024, China*
[3]*School of Mechanics and Engineering, Liaoning Technical University, Fuxin 123000, China*

Correspondence should be addressed to Tianhui Ma; tianhuima@dlut.edu.cn

Received 17 March 2018; Accepted 3 July 2018; Published 17 July 2018

Academic Editor: Wei Wu

Based on the existing Canadian ESG microseismic monitoring system, a mobile microseismic monitoring system for a soft rock tunnel has been successfully constructed through continuous exploration and improvement to study the large-scale nucleation and development of microfractures in the soft rock of the Yangshan Tunnel. All-weather, continuous real-time monitoring is conducted while the tunnel is excavated through drilling and blasting, and the waveform characteristics of microseismic events are analysed. Through the recorded microseismic monitoring data, the variation characteristics of various parameters (e.g., the temporal, spatial, and magnitude distributions of the microseismic events, the frequency of microseismic events, and the microseismic event density and energy) are separately studied during the process of large-scale deformation instability and failure of the soft rock tunnel. The relationship between the deterioration of the rock mass and the microseismic activity during this failure process is consequently discussed. The research results show that a microseismic monitoring system can be used to detect precursors; namely, the microseismic event frequency and energy both will appear "lull" and "active" periods during the whole failure process of soft rock tunnel. Two peaks are observed during the evolution of failure. When the second peak occurs, it is accompanied by the destruction of the surrounding rock. The extent and strength of the damage within the surrounding rock can be delineated by the spatial, temporal, and magnitude distributions of the microseismic events and a microseismic event density nephogram. The results of microseismic analysis confirm that a microseismic monitoring system can be used to monitor the large-scale deformation and failure processes of a soft rock tunnel and provide early warning for on-site construction workers to ensure the smooth development of the project.

1. Introduction

Rock is an anisotropic and nonhomogeneous material. When cracks within rock germinate, expand, and ultimately penetrate, the internal accumulation strain energy is released in the form of waves, resulting in microseismic events [1–5]. Microseismic monitoring technology can be employed to collect and analyse microseismic events, the data from which can be used to invert the time, location, and magnitude of microseismic event and predict the possibility, energy, and position of large-scale deformation and failure of soft rock tunnels [6–8].

Microseismic monitoring, which is a type of passive monitoring technology, can be utilized for the long-term monitoring and short-term prediction of microseismic activity within underground structures, and it has been widely adopted in mining engineering and other engineering fields [9–15]. McCreary et al. [16] used a 16-channel Electrolab MP250 microseismic system to resolve the occurrence of rockbursts in a small gold mine. Microseismic monitoring was also employed along the left bank slope of the Jinping-I Hydropower Station to analyse the stability of the slope and investigate the deformation of deep rock masses in particular [17]. Furthermore, Ma et al. [18] utilized microseismic monitoring technology to reveal the spatial and temporal variations in microseismic and rockburst activities in deep-buried tunnels for the Jinping-II Hydropower Station.

Microseismic monitoring technology is being applied with increasing frequency to various projects at present, but

it is the first time that it has been applied to a soft rock tunnel for the monitoring and early warning of soft rock instability and failure in the world. Therefore, there are no successful monitoring and warning experiments to learn directly. Based on the Canadian Engineering Seismology Group (ESG) microseismic monitoring system, a mobile microseismic monitoring system was successfully constructed and applied to a soft rock tunnel for continuous exploration and improvement. This paper analyses the signal characteristics of various events and extracts the amplitude-frequency characteristics of microseismic event waveforms. Based on a combination of the temporal, spatial, and magnitude distributions of microseismic events and the microseismic event density nephogram, the timing, intensity, and extent of large-scale deformation and failure within the soft rock tunnel can be noted with the temporal variations in the microseismic events and microseismic energy. The findings can provide strong guarantees for safe tunnel construction and production management.

2. Engineering Background

The Yangshan Tunnel is located in a hilly area of the Loess Plateau of North Shanxi Province. The total length of the tunnel is 11668.3 m with a maximum burial depth of 277.07 m, and large-scale deformation and instability failure of the soft rock are evident in some places throughout the tunnel. The Yangshan Tunnel area is geotectonically situated within the southeastern corner of the Erdos Basin. The host rock of the tunnel is composed of interbedded sandstone and mudstone. A collapsible sandy loess has been found in the DK382 + 970~DK385 + 200 area of the tunnel with a collapsibility coefficient of $\delta s = 0.015 \sim 0.065$, based upon which it is classified as a medium collapsible loess belonging to a grade II (medium) self-weight collapsible site. It exhibits two major characteristics when the loess tunnel is constructed. The first characteristic is that, following the excavation of the loess tunnel, the concentration of stress on the vault and the part is excessively large. These stresses resulted in substantial settling of the vault and the instability of the tunnel structure, leading to the occurrence of landslides. The second characteristic is that the collapsible loess basement hosting the tunnel is easily destroyed by water, leading to a decline in the foundation bearing capacity.

3. Microseismic Monitoring System for a Soft Rock Tunnel

3.1. Microseismic Monitoring Principle. Microseismic activity is essentially a process of the continuous accumulation and intermittent release of stress [19, 20]. Within the larger scope of engineering standards, the generation and expansion of rock fractures are accompanied by the rapid release and propagation of elastic waves within the surrounding rock mass [21, 22], those elastic waves propagating through the rock are received by the velocity sensors of different positions, and the microseismic events are located by the time difference of propagation [23, 24]. The principle used for the positioning of a microseismic event is shown in Figure 1. The microseismic signals contain a vast quantity of information related to rockbursts, following which an interpretation of the abovementioned information can be used to analyse the fracturing and instability of the rock.

3.2. Microseismic Monitoring System Construction. The correct construction of the microseismic monitoring system is an important step in the entire microseismic monitoring process, and it is also a prerequisite for normal microseismic monitoring [24–26]. This project adopts an improved high-precision microseismic monitoring system produced by ESG Solutions in Canada to monitor and analyse microfractures within the rock mass during the tunnel excavation throughout the day. The system mainly includes six uniaxial velocity sensors, a digital signal acquisition system, and a digital signal processing system (Figure 2). The ESG digital signal acquisition system, which is connected to the sensor through an unshielded cable, is an important device that converts the electrical signal to a digital signal. However, excessively increasing the length of the connecting cable will greatly increase the cost and simultaneously attenuate the signal with increasing severity. Therefore, to ensure normal transmission of the signal, the acquisition system cannot be installed more than 300 m from the sensor. However, for the sake of safety, the equipment should not be installed too close to the face of the tunnel. Therefore, the equipment should be installed at a distance of approximately 130 m away from the working face, and the sensors will be moved by adding cable as the working face advances forward during the monitoring process. The acquisition equipment should be moved forward when the length of the cable between the rearmost sensor and digital signal acquisition system is longer than 250 m. To locate microseismic events with a greater accuracy, it is necessary to ensure that no fewer than 6 sensors are operating normally. In this monitoring scheme, 3 sensors are arranged on either side of the tunnel, and the distance between adjacent sensors must be approximately 25 m. Meanwhile, the distance between the first two sensors and the working face should be within 50 m, otherwise the microseism positioning accuracy will be affected.

3.3. Analysis and Recognition of Various Event Waveforms. When microseismic monitoring technology is properly employed to perform real-time monitoring and effectively analyse the instability and failure of a tunnel rock mass, one key step is that monitoring man can quickly and effectively distinguish microseismic events from a large number of noise disturbances [27–29]. Therefore, the correct identification of the microseism waveform is an important component of microseismic monitoring and forecasting [30, 31]. The following types of waveforms should be distinguished during the process of soft rock tunnel excavation via drilling and blasting (Figure 3).

3.3.1. Blast Event Waveform. The voltage amplitude of a blast waveform ranges approximately from −5 to 5 V. The associated waveform is relatively neat with a high amplitude

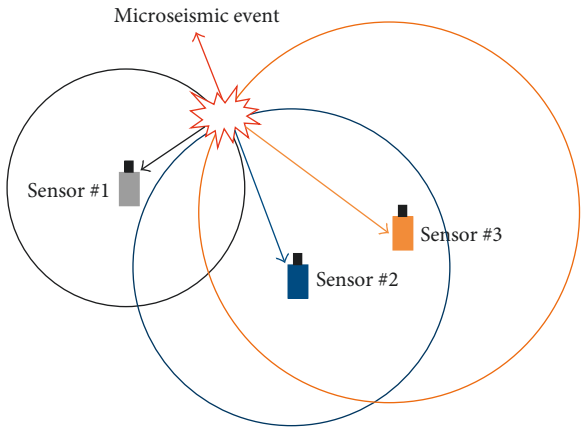

Figure 1: Schematic diagram of the positioning principle for microseismic events.

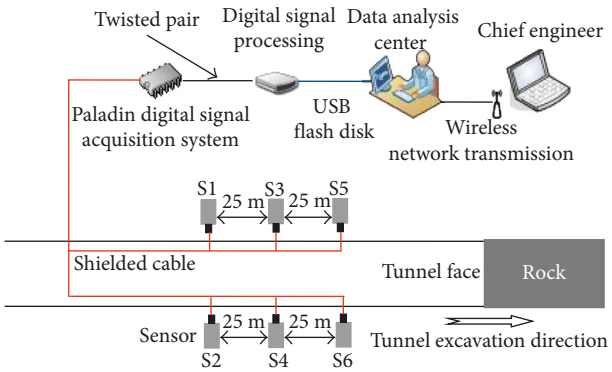

Figure 2: Complete schematic diagram of the sensor arrangement and the data acquisition, transmission, and processing in the microseismic monitoring system.

and long wavelength cycle, and the wave attenuates relatively slowly.

3.3.2. Microseismic Event Waveform. The amplitude of a microseismic waveform is small. Furthermore, the waveform attenuates slowly, and the coda wave is more developed; the voltage amplitude fluctuates between −0.05 and 0.05 V. The P wave of a microseismic event arrives before the S wave. When the S wave arrives, the amplitude of voltage evidently increases due to the superposition of the P wave and the S wave. The arrival times of the two waves can be clearly distinguished within the waveform diagram.

3.3.3. Large Machine Impact Tunnel Waveform. The waveform is transient and rapidly attenuates. The duration of the waveform is no more than 10 ms, and the voltage amplitude fluctuates from −1 to 1 V.

3.3.4. Electrical Current Interference Waveform. The waveform of this type of signal has an obvious vertical asymmetry that is very easy to identify.

4. Microseismic Activity Characteristic Analysis

4.1. Characteristics of the Temporal, Spatial, and Magnitude Distributions of Microseismic Activity. The temporal, spatial, and magnitude distributions of microseismic activity during the excavation of the soft rock tunnel by drilling and blasting are shown in Figure 4, in which each circle represents a microseismic event, the diameter of each circle represents the energy level of the microseismic event, and the different colours of the circles represent different magnitudes (i.e., red indicates the largest magnitude and purple indicates the lowest magnitude).

The microseismic events that occurred within the tunnel rock mass from November 4 to November 7, 2017, exhibited low energies and small magnitudes, and they were fewer in quantity with a more discrete distribution (Figure 4(a)). The surrounding tunnel rock was less affected by the excavation disturbance, the integrity of the surrounding rock was good, and there was no obvious deformation of the surrounding rock. The number of microseisms increased slightly from November 8 to November 10, but the microseism magnitudes were small (as shown in Figure 4(b)). Furthermore, there was no significant concentration of microseismic events. Although the magnitudes of the microseismic events were not high from November 11 to November 12, the number of microseismic events clearly increased, and a greater amount of energy was released within the surrounding rock. There was some evidence of the nucleation of microseismic events within the range delineated with an ellipse in Figure 4(c). In conjunction with a field investigation, the roof of the surrounding rock appeared to be macroscopical visible deformation. The microseismic events that occurred on November 13-14 were characterized by not only a greater quantity but also a concentrated distribution, thereby forming an intensive area of microseismic activity in which three events with relatively large magnitudes and high energies occurred (Figure 4(d)). As a consequence, the deformation of the surrounding rock roof intensified during this period, resulting in collapse (Figure 5). However, since the maximum microseismic magnitude was only −1.53 and the total amount of energy released by the surrounding rock was not high, the strength of the failure of the roof was relatively low; therefore, the roof was damaged to a limited extent without causing casualties or equipment damage.

4.2. Frequency Evolution Law of the Microseismic Events. The processes of large-scale deformation and failure of a soft rock tunnel are essentially identical to the dynamic evolution processes of microfractures inside a rock. Microseismicity is the release of strain energy in the form of elastic waves when a microfracture is generated, and the frequency changes in microseismic events are closely related to the microfractures produced within the rock after it is disturbed during excavation [32]. Therefore, the temporal variations in the frequency of microseismic activity recorded by the microseismic monitoring system can effectively reflect the changes in the large-scale deformation failure and stress field of the soft rock. Accordingly, a typical case of failure of the soft

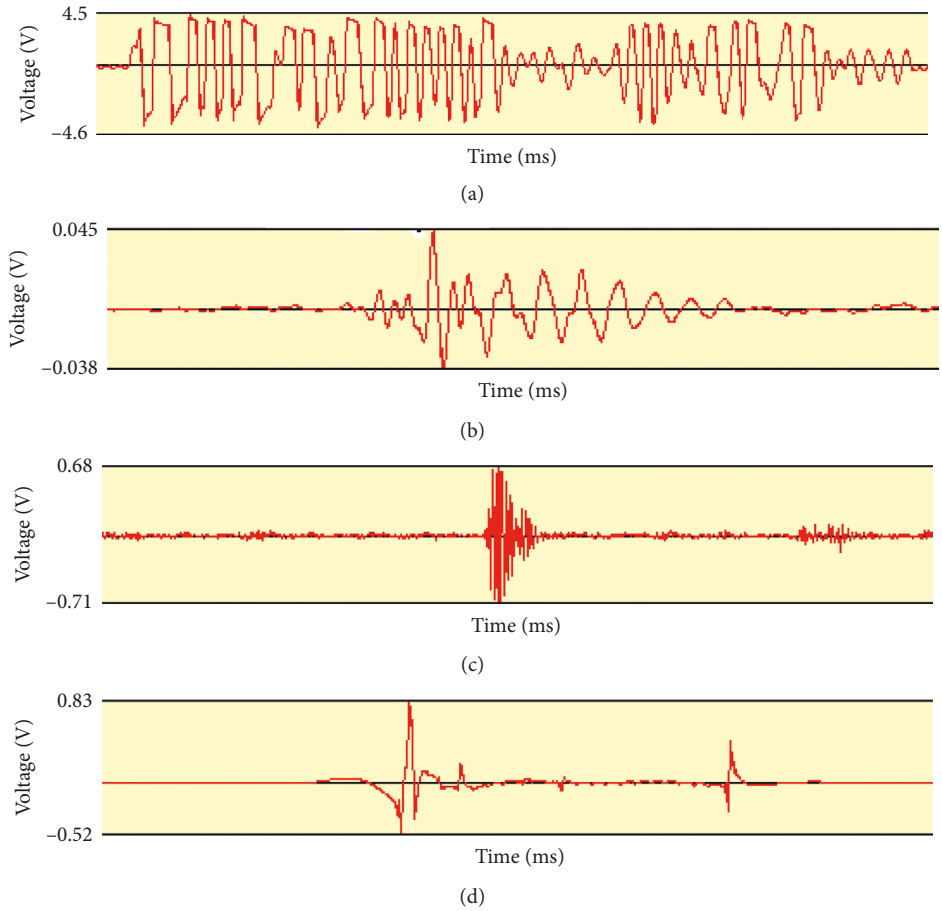

Figure 3: Various event waveforms. (a) Blast event waveform, (b) microseismic event waveform, (c) large machine impact tunnel waveform, and (d) electrical current interference waveform.

rock tunnel is selected as the research object to study the inherent relationship between the stress and the microseismic events that occurred during the large-scale deformation and failure of the soft rock tunnel and analyse the evolution of microseismic activity. Only 5 microseismic events occurred over the 3-day period from November 4 to November 6, 2017, and the surrounding rock was relatively less affected by excavation and unloading. Meanwhile, the microseismic activity was more frequent on November 7-8, during which period 13 microseismic events were detected. The microseismic activity rate decreased from November 9 to November 10. There was a peak in the number of microseismic events between November 4 and November 10 (Figure 6). However, the stress of the surrounding rock was self-adaptive and in a relatively quiet period; consequently, there was no obvious large-scale deformation in the surrounding tunnel rock. This indicates that the local stress in the rock mass was constantly adjusting and accumulating during this time period. On November 11-12, the number of microseismic events increased rapidly, a total of 19 microseisms occurred within the surrounding rock within the two-day period, the number of daily microseismic events was greater than that of the previous period, the stress concentration in the rock mass was correspondingly obvious, and an area of large-scale deformation appeared within the rock mass, and this indicated the occurrence of soft rock failure. The number of microseismic events on November 13 showed a slight decline, but it was still relatively high, indicating that the stresses in the surrounding rock stress were not fully released and that the possibility of surrounding rock failure was still high. With the ongoing excavation of the tunnel, the total number of microseismic events increased on November 14 and reached a maximum of 11 events; this indicated that the continuous action of external forces caused severe deterioration of the mechanical properties of the surrounding rock and a decrease in the strength of the rock mass; the deformation of the soft rock developed to an extreme state, which finally led to the collapse of the roof of the surrounding rock. The frequency of microseismic events decreased from November 15 to November 18, and the stress of the rock mass redistributed after the roof collapsed, resulting in a microseismic lull.

4.3. Evolution Law of the Microseismic Energy. Analysing the temporal distribution law of the energy released during the microfractures within the rock mass of a soft rock tunnel project is an effective way to study the development process of large-scale deformation in the rock mass [33]. From November 4 to November 6, 2017, the energy released within

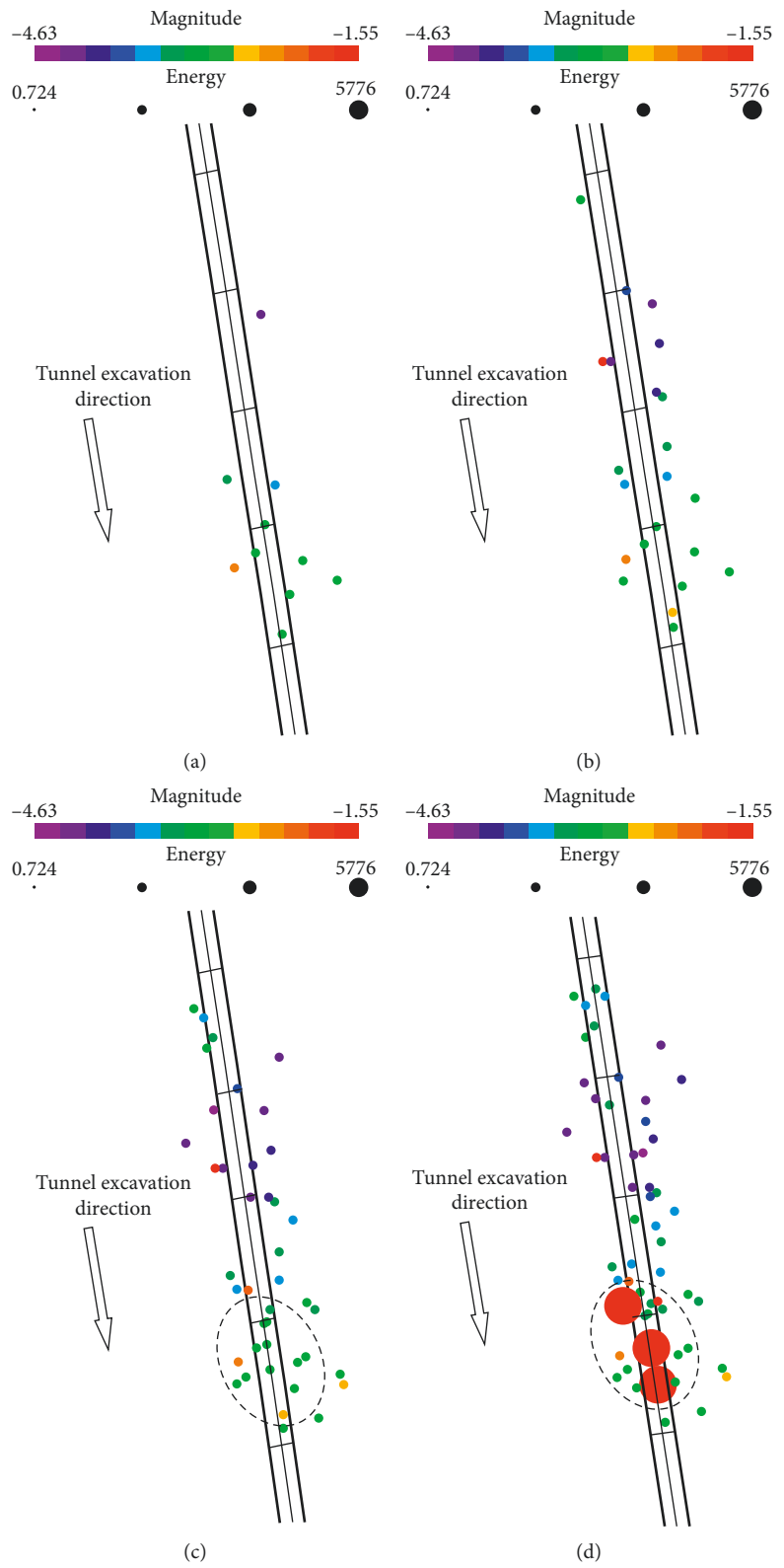

Figure 4: Schematic diagrams of the temporal, spatial, and magnitude distributions of microseismic activity during the excavation of the tunnel by drilling and blasting. (a) Distribution map of microseismic events on 4~7 November 2017, (b) distribution map of microseismic events on 4~10 November 2017, (c) distribution map of microseismic events on 4~12 November 2017, and (d) distribution map of microseismic events on 4~14 November 2017.

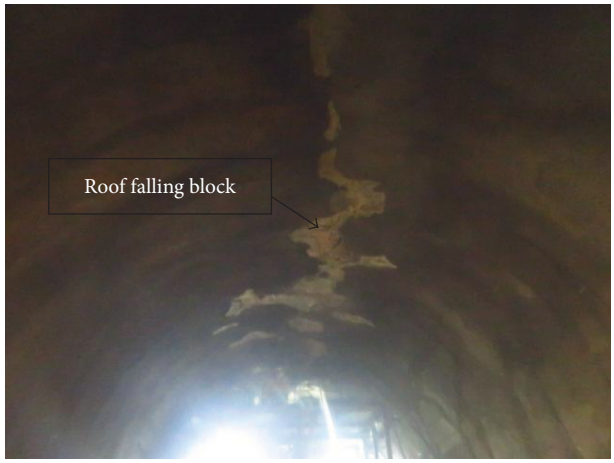

Figure 5: Large-scale deformation and failure of the surrounding rock roof.

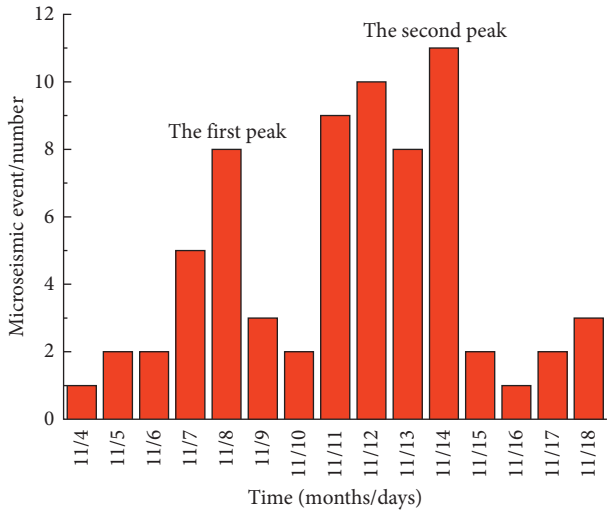

Figure 6: The evolution of the number of microseismic events with time during the large-scale deformation and failure of the soft rock.

the surrounding rock was in a relatively gentle state, and it was maintained at a relatively low level (Figure 7). From November 7 to November 10, the energy released from the surrounding rock abruptly increased and then decreased sharply. The cause of this rise in the energy released from the surrounding rock was the influence of disturbances to the rock mass by drilling and blasting. Moreover, the secondary stress field of the surrounding rock did not adjust to an equilibrium state and was subjected to an external load again, additional cracks further germinated in the rock and expanded, and they were accompanied by the massive release of energy within the surrounding rock. Subsequently, the energy released from the surrounding rock decreased, and this phase can be initially judged as the "quiet period" before the large-scale deformation and failure of the surrounding rock. As expected, the energy released from the microfractures of the rock mass as it continued to rise from November 11 to November 14. With the ongoing excavation of the tunnel, the stress concentration of the rock mass

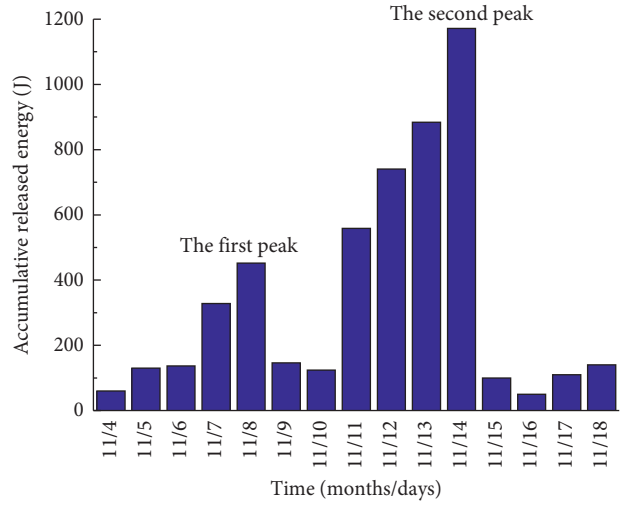

Figure 7: Evolution law of the microseismic energy with time during the large-scale deformation and failure process of soft rock.

became aggravated, resulting in the continuous development of existing microcracks simultaneous with the constant accumulation and transfer of strain energy. Consequently, on November 14, the release of microseismic energy reached a peak, following which the roof of the surrounding rock began to fall on that day. Due to the immense release of energy on November 14 coincident with the damage to the surrounding rock, the energy released from the surrounding rock rapidly decreased from November 15 to 18.

5. Results and Discussion

As shown in Figures 6 and 7, the changes in the microseismic event frequencies with time were basically the same as those of the microseismic energy, both experienced microseismic lulls and active periods, and there were two peaks in their temporal profiles. The microseismic activity was quieter in the short periods both before and after the first peak. The microseismic activity before the second peak continued to rise, and the stress and energy adjustments within the surrounding rock were the most dramatic, resulting in a stress concentration in the surrounding rock that led to the germination, expansion, and coalescence of cracks within the rock mass, thereby weakening the integrity and bearing capacity of the surrounding rock. As a consequence, the roof suffered from large-scale deformation that indicated the instability and failure of the soft rock tunnel when the number and energy of microseismic events reached their second peak, and the roof of the surrounding rock was destroyed.

A microseismic event density nephogram can reveal the degree to which microseismic events aggregate within a certain period of time and within a certain range (Figure 8). Based on different colours, the probability of geological disaster ranges from high to low in succession from red to yellow to green and then blue. Blue areas correspond to absolute safety, while red areas denote the most concentrated distribution of microseismic events (i.e., the largest microseismic event density). Therefore, red areas predict the

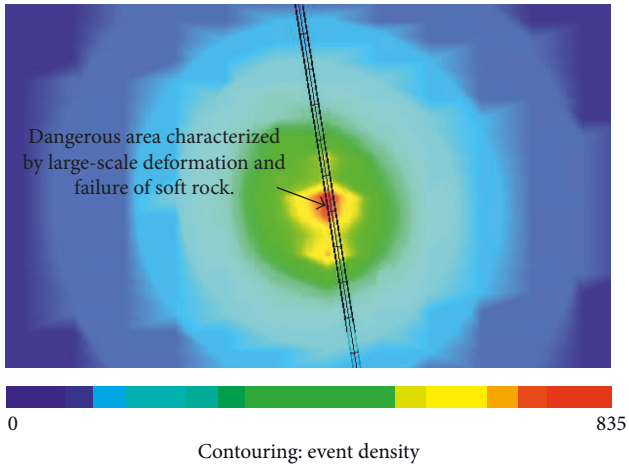

Figure 8: Microseismic event density nephogram at the time of soft rock failure.

regions (i.e., dangerous areas) of soft rock that will experience large-scale deformation and damage. Combining a microseismic event density nephogram with the spatial, temporal, and magnitude distributions of microseismic events, the range of large-scale deformation and damage and the strength of the soft rock tunnel can be determined.

Through the variations in the frequencies and energies of the microseismic events over time, it is possible to fully explain the internal damage processes of the rock mass and determine the timing of the destruction of the surrounding rock. The extent of damage and strength of the surrounding rock can be delineated by the spatial, temporal, and magnitude distributions of the microseismic events and the microseismic event density nephogram. Predictions of the time, location, and magnitude of a disaster can provide early warning for the construction workers. At the same time, based on the discussion in this paper, we can use a microseismic monitoring system to monitor the entire large-scale deformation and instability failure process of a soft rock tunnel.

6. Conclusion

This paper examines the large-scale deformation and failure of the rock mass surrounding the Yangshan Tunnel through the use of microseismic monitoring technology to continually investigate soft rock deformation and failure. The relationships among the temporal and spatial evolutionary processes of the microseismicity and the large-scale deformation and failure of the soft rock are studied by comparing the actual situation in the field with the results of microseismic monitoring, and several research conclusions can be drawn:

(1) The first microseismic real-time monitoring system has already been constructed to monitor the large-scale deformation and failure of soft rock in railway tunnels in the world. Combined with information regarding the construction conditions, the amplitude-frequency characteristics of different vibration waveforms can be analysed, and the characteristics of microseismic waveforms propagating through a rock mass can be obtained.

(2) The changes in the number of microseismic events and their energies are consistent in time, and these two curves over time basically experience two peaks. The period of time when both the number and the energy of microseisms reach their second peak can be considered the moment of disaster in the soft rock tunnel. Moreover, the rough extent and strength of damage within the soft rock tunnel can be delineated by the spatial, temporal, and magnitude distributions of the microseismic events and a microseismic event density nephogram.

(3) Microseismic events in a rock mass have both temporal precedence and spatial consistency with the large-scale deformation and failure of soft rock. This proves that the large-scale deformation and failure processes within a soft rock tunnel can be monitored. The results of such monitoring could provide effective guidance for the improvement of on-site support measures, ensure the safety of on-site workers and construction equipment, and ensure the smooth progress of the project. At the same time, it could provide a successful example for the microseismic monitoring of similar projects.

Data Availability

The data used to support the findings of this study are available from the corresponding author upon request.

Conflicts of Interest

The authors declare that they have no conflicts of interest.

Acknowledgments

This study was supported by the National Key Basic Research Development Plan (973) (no. 2014CB047100) and the Chinese National Natural Science Foundation (nos. 51627804, 41572249, and 51579031).

References

[1] D. Amitrano, "Rupture by damage accumulation in rocks," *International Journal of Fracture*, vol. 139, no. 3-4, pp. 369–381, 2007.

[2] A. P. Bunger, J. Kear, A. V. Dyskin, and E. Pasternak, "Sustained acoustic emissions following tensile crack propagation in a crystalline rock," *International Journal of Fracture*, vol. 193, no. 1, pp. 87–98, 2015.

[3] K. Ma, C. A. Tang, Z. Z. Liang, D. Y. Zhuang, and Q. B. Zhang, "Stability analysis and reinforcement evaluation of high-steep rock slope by microseismic monitoring," *Engineering Geology*, vol. 218, pp. 22–38, 2017.

[4] M. Cai, P. K. Kaiser, and C. D. Martin, "Quantification of rock mass damage in underground excavations from microseismic event monitoring," *International Journal of Rock Mechanics and Mining Sciences*, vol. 38, no. 8, pp. 1135–1145, 2001.

[5] D. A. J. Mendecki, *Seismic Monitoring in Mines*, Chapman and Hall, London, UK, 1997.

[6] W. Cai, L. Dou, Z. Li, J. He, H. He, and Y. Ding, "Mechanical initiation and propagation mechanism of a thrust fault: a case study of the Yima section of the XIASHI-yima thrust (north side of the Eastern Qinling Orogen, China)," *Rock Mechanics and Rock Engineering*, vol. 48, no. 5, pp. 1927–1945, 2015.

[7] D. A. J. Mendecki, "Real time quantitative seismology in mines," in *Proceedings of the International Symposium on Rockbursts and Seismicity in Mines*, Kingston, ON, Canada, August 1993.

[8] A. M. Milev, S. M. Spottiswoode, A. J. Rorke, and G. J. Finnie, "Seismic monitoring of a simulated rockburst on a wall of an underground tunnel," *Journal of South African Institute of Mining and Metallurgy*, vol. 101, no. 5, pp. 253–260, 2001.

[9] T. I. Urbancic and C. I. Trifu, "Recent advances in seismic monitoring technology at Canadian mines," *Journal of Applied Geophysics*, vol. 45, no. 4, pp. 225–237, 2000.

[10] J. R. Zhou, T. H. Yang, P. H. Zhang, T. Xu, and J. Wei, "Formation process and mechanism of seepage channels around grout curtain from microseismic monitoring: a case study of Zhangmatun iron mine, China," *Experimental Gerontology*, vol. 226, pp. 301–315, 2017.

[11] C. Tang, J. Wang, and J. Zhang, "Preliminary engineering application of microseismic monitoring technique to rockburst prediction in tunneling of Jinping II project," *Journal of Rock Mechanics and Geotechnical Engineering*, vol. 2, no. 3, pp. 193–208, 2010.

[12] A. Leśniak and Z. Isakow, "Space–time clustering of seismic events and hazard assessment in the Zabrze-Bielszowice coal mine, Poland," *International Journal of Rock Mechanics and Mining Sciences*, vol. 46, no. 5, pp. 918–928, 2009.

[13] A. Hirata, Y. Kameoka, and T. Hirano, "Safety management based on detection of possible rock bursts by AE monitoring during tunnel excavation," *Rock Mechanics and Rock Engineering*, vol. 40, no. 6, pp. 563–576, 2007.

[14] S. L. Li, X. G. Yin, W. D. Zheng, and C. Trifu, "Research of multi-channel microseismic monitoring system and its application to Fankou lead-zinc mine," *Chinese Journal of Rock Mechanics and Engineering*, vol. 24, no. 12, pp. 2048–2053, 2005.

[15] X. Luo, J. Ross, P. Hatherly, B. Shen, and M. D. Fama, "Microseismic monitoring of highwall mining stability at Moura Mine, Australia," *Exploration Geophysics*, vol. 32, no. 4, pp. 340–345, 2001.

[16] R. McCreary, J. McGaughey, Y. Potvin et al., "Results from microseismic monitoring, conventional instrumentation, and tomography surveys in the creation and thinning of a burst-prone sill pillar," *Pure and Applied Geophysics*, vol. 139, no. 3-4, pp. 349–373, 1992.

[17] N. W. Xu, C. A. Tang, L. C. Li et al., "Microseismic monitoring and stability analysis of the left bank slope in Jinping first stage hydropower station in Southwestern China," *International Journal of Rock Mechanics and Mining Sciences*, vol. 48, no. 6, pp. 950–963, 2011.

[18] T. H. Ma, C. A. Tang, L. X. Tang, W. D. Zhang, and L. Wang, "Rockburst characteristics and microseismic monitoring of deep-buried tunnels for Jinping II hydropower station," *Tunnelling and Underground Space Technology*, vol. 49, pp. 345–368, 2015.

[19] C. A. Tang and P. K. Kaiser, "Numerical simulation of cumulative damage and seismic energy release during brittle rock failure—part I: fundamentals," *International Journal of Rock Mechanics and Mining Sciences*, vol. 35, no. 2, pp. 113–121, 1998.

[20] H. Wang and M. Ge, "Acoustic emission/microseismic source location analysis for a limestone mine exhibiting high horizontal stresses," *International Journal of Rock Mechanics and Mining Sciences*, vol. 45, no. 5, pp. 720–728, 2008.

[21] A. McGarr, S. M. Spottiswoode, N. C. Gayand, and W. D. Ortlepp, "Observations relevant to seismic driving stress, stress drop, and efficiency," *Journal of Geophysical Research Solid Earth*, vol. 84, no. B5, pp. 2251–2261, 1979.

[22] W. S. Zhu and J. Zhao, *Stability Analysis and Modelling of Underground Excavations in Fractured Rocks*, Elsevier, New York, NY, USA, 2004.

[23] S. J. Gibowicz, "Seismicity induced by mining," *Advances in Geophysics*, vol. 32, pp. 1–74, 1990.

[24] S. L. Li, "Discussion on microseismic monitoring technology and its applications to underground projects," *Chinese Journal of Underground Space and Engineering*, vol. 5, no. 1, pp. 122–128, 2009.

[25] M. Ge, "Efficient mine microseismic monitoring," *International Journal of Coal Geology*, vol. 64, no. 1-2, pp. 44–56, 2005.

[26] C. A. Tang and J. M. Wang, "Rock and seismic monitoring and prediction–the feasibility and the preliminary practice," *Rock Mechanics and Engineering News*, vol. 89, no. 1, pp. 43–55, 2010.

[27] D. A. Angus, A. Aljaafari, P. Usher, and J. P. Verdon, "Seismic waveforms and velocity model heterogeneity: towards a full-waveform microseismic location algorithm," *Journal of Applied Geophysics*, vol. 111, pp. 228–233, 2014.

[28] C. Huang, L. Dong, Y. Liu, and J. Yang, "Acoustic wave-equation based full-waveform microseismic source location using improved scattering-integral approach," *Geophysical Journal International*, vol. 209, no. 3, pp. 1476–1488, 2017.

[29] O. J. Michel and I. Tsvankin, "Waveform inversion for microseismic velocity analysis and event location in VTI media," *Geophysics*, vol. 82, no. 4, pp. WA95–WA103, 2017.

[30] S. Arrowsmith and L. Eisner, "A technique for identifying microseismic multiplets and application to the Valhall field, North Sea," *Geophysics*, vol. 71, no. 2, pp. V31–V40, 2006.

[31] S. Cesca and F. Grigoli, "Full waveform seismological advances for microseismic monitoring," *Advances in Geophysics*, vol. 56, pp. 169–228, 2015.

[32] E. Hoek and E. T. Brown, *Underground Excavations in Rock*, The Institution of Mining and Metallurgy, London, UK, 1980.

[33] D. A. Beck and B. H. G. Brady, "Evaluation and application of controlling parameters for seismic events in hard-rock mines," *International Journal of Rock Mechanics and Mining Sciences*, vol. 39, no. 5, pp. 633–642, 2002.